TRANSONIC FLIGHT AND MOVABLE LOAD MODELLING FOR WING-BOX PRELIMINARY SIZING

Paul Lancelot and Roeland De Breuker

Delft University of Technology
South Holland, Netherlands
P.M.G.J.Lancelot@tudelft.nl
R.DeBreuker@tudelft.nl

Keywords: aeroelasticity, structural sizing, gust loads, control surfaces, aerodynamic characterisation

Abstract: In this paper, a methodology is presented to size an aircraft wing-box accounting for steady and dynamic loads combined with active control. Several aerodynamic corrections are used and benchmarked to ensure a consistent level of fidelity during the load analysis. Reduced order models (ROM) of the aircraft movables, gust loads and maneuvers loads are derived from rigid CFD analysis and used as substitutes for the loads in the aeroelastic simulation.

1 INTRODUCTION

The quest to reduce fuel consumption has led the aircraft industry to develop new strategies to decrease aero-structures weight. In order to do so, control surfaces are used for active load alleviation. However, the actual weight saving may only be evaluated once the airframe is sized for the large number of load cases it will have to withstand during service life. The final design also needs to comply with the many requirements for flight performances, safety, and handling qualities.

The sizing process mostly relies on panel codes (doublet lattice, vortex lattice, etc.) as they are relatively accurate and yet very fast. However, they are limited to linear flow conditions, and transonic shock or flow separation cannot be simulated with such methods. In these conditions, the load alleviation and manoeuvring capabilities of control surfaces will also be affected. This means that a significant part of the sizing load cases for a regular passenger aircraft cannot be approximated with satisfying accuracy, leading to over-conservative load assumptions and generally heavier design. On the other hand, computational fluid dynamics with Reynolds averaged Navier-Stokes (CFD-RANS) analysis, is capable of approximating flight loads under transonic and detached flow regime with higher fidelity. The computational time required for such simulations is nevertheless too long to be efficiently included in the sizing process of the airframe and is usually restricted to validation purposes only.

The proposed approach in this paper aims to bring the accuracy of CFD to quick linear aeroelastic simulations for structural sizing. This is achieved by deriving reduced order models (ROM) of the aircraft movables, gust loads and manoeuvres loads from rigid CFD analysis and using these as substitutes for the loads in the aeroelastic simulation. The goal of this methodology is to remain non-intrusive and easily compatible with commercial analysis and optimisation tool such as NASTRAN. Building a fast aerodynamic model of the control surfaces also allows quick control optimisation, to evaluate their load alleviation potential, which can also affect the sizing of the wing box. The corrected loads can then be incorporated into the wing-box sizing process, which relies on a gradient-based optimizer that will eventually

determine the optimal stiffness and thickness distribution of the wing structure. Although only one configuration is evaluated in the present work, the methodology developed here aims to facilitate the wing layout design process.

2 STEADY AERODYNAMIC LOAD CORRECTION FOR THE WING AND MOVEABLE

Various approaches have been developed to perform suitable load corrections, but none is universal and usually case dependent. *Dillinger et al.* [1] used Euler CFD simulations to correct steady manoeuvre loads obtained with the DLM code embedded in NASTRAN. More recently, MSC Software implemented in NASTRAN the hybrid static approach (HSA), which replaces the rigid aerodynamic contribution of the wing with higher order CFD results stored in a database [2]. This method simplifies the load correction process and only requires the corrections to be computed once. The rigid aerodynamic databases can also be swapped for different flow conditions. Aeroelastic effects are captured using the DLM method, which allows NASTRAN to retain its capability to compute steady aeroelastic sensitivities. It has been used by *Bordogna et al.* to size a wing-box [3]. The method is illustrated in Figure 1.

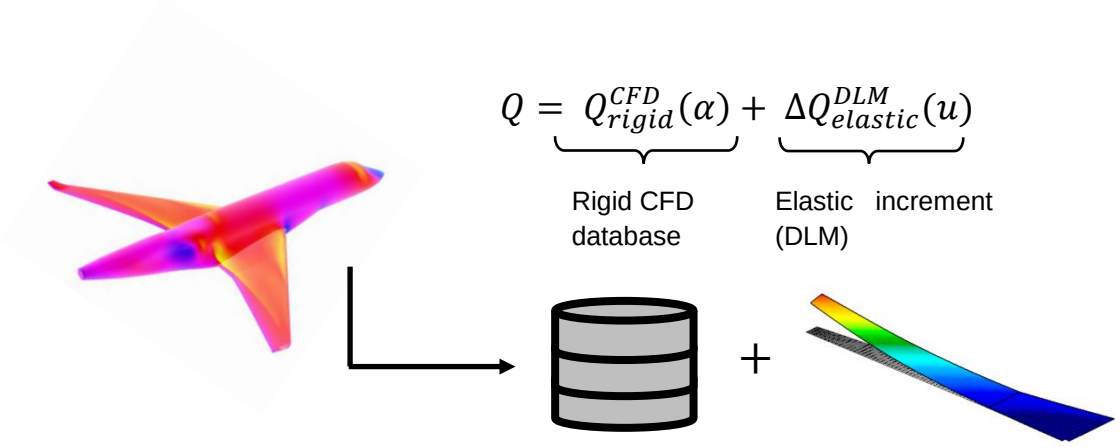

Figure 1: Schematic of the Hybrid Static Approach (HSA) implemented inside MSC NASTRAN.

To demonstrate the validity of this approach, we compared it against a coupled CFD/CSM high-fidelity solution. A NASTRAN aeroelastic model of a generic high-speed business jet is used in conjunction with an outer shell model for the CFD. The aeroelastic model, shown in Figure 2 is built of 1200 shell elements (CQUAD4 and CTRIA3) 650 beam elements (CBEAM, for the stiffeners) and 60 lump mass elements (CONM2). There are a total of 970 grid points. To improve the computational, time rigid elements (RBE2 and RBE3) are used to reduce the number of degrees of freedom (DOF). Finally, doublet lattice panels (DLM) to compute the aerodynamic loads are splined onto the structure.

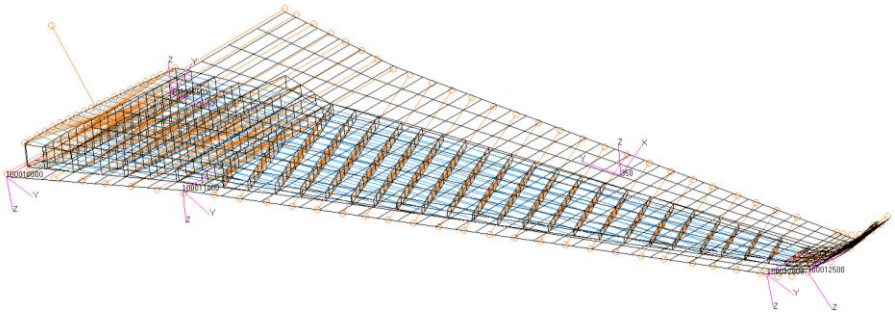

Figure 2: Generic business jet aeroelastic model. The fuselage and the tail are not shown on this image.

The CFD simulations are performed using the Ansys Fluent solver using the two equations k-ω turbulence model for steady and unsteady simulations. A RANS model is chosen because it provides viscous effects, as opposed to Euler and other lower fidelity models. The grid used for the simulations is composed of 10 million unstructured cells. As shown in Figure 3, only half of the aircraft is modelled, using a symmetric boundary condition, because only symmetric manoeuvres are considered.

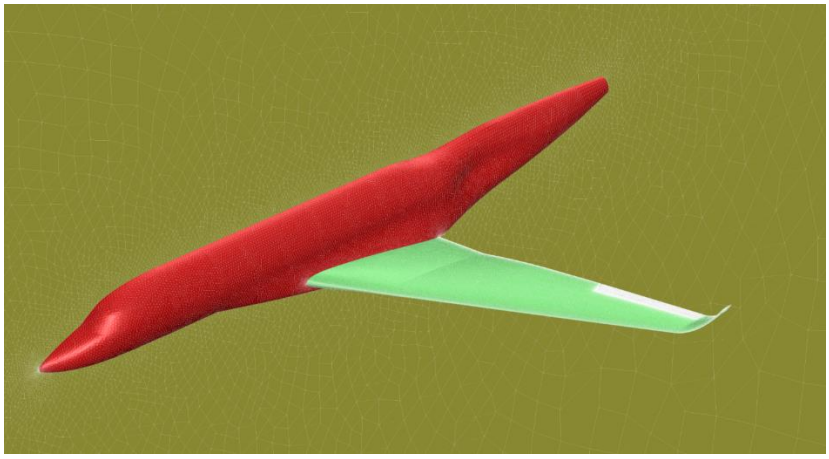

Figure 3: CFD grid of the generic business jet. A tail was also added.

For this comparison, the aircraft is flown at Mach 0.85 with a dynamic pressure of 15000 Pa and angle of attacks (AoA) ranging from -5 to +7 degrees. Only two CFD simulations, at zero and one degree of AoA, are needed to build the HSA correction database. The NASTRAN solver is then able to extrapolate the rigid lift contribution using these two points linearly. The correction is only valid for one Mach and dynamic pressure combination, and additional rigid CFD analysis may be required to cover other parts of the flight envelope. HSA method still relies on the DLM panel method but only to capture loads increment due to wing flexibility. Results of the comparison between the HSA method and the coupled CFD/CSM high-fidelity are shown in Figure 5. Results of a non-corrected DLM panel method solution are also added to the comparison.

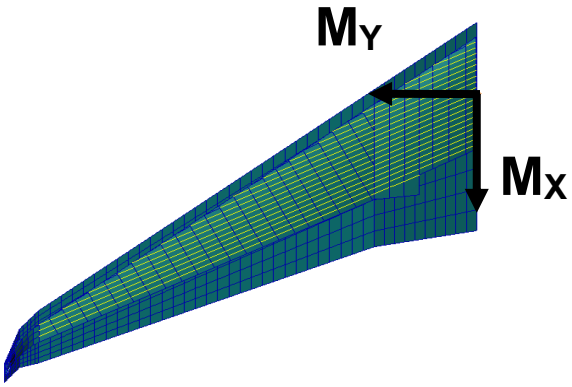

Figure 4: M_X and M_Y moments are measured at the wing root around the x and y-axes, respectively.

The lift, tip displacement and wing root moments around the x and y-axes (as shown above in Figure 4) are compared. Figure 5 shows good agreement within 5% for most responses between the high fidelity coupled CFD/CSM solution and the HSA method running with NASTRAN. The non-corrected DLM method, also running with NASTRAN, shows significant discrepancies, for a run time barely shorter than with the HSA method. We also note a rather linear behaviour of the elastic wing compared to the rigid CFD simulation. This implies that flexibility effects can lead to a system simplification as already observed by *Schewe and Mai* [4].

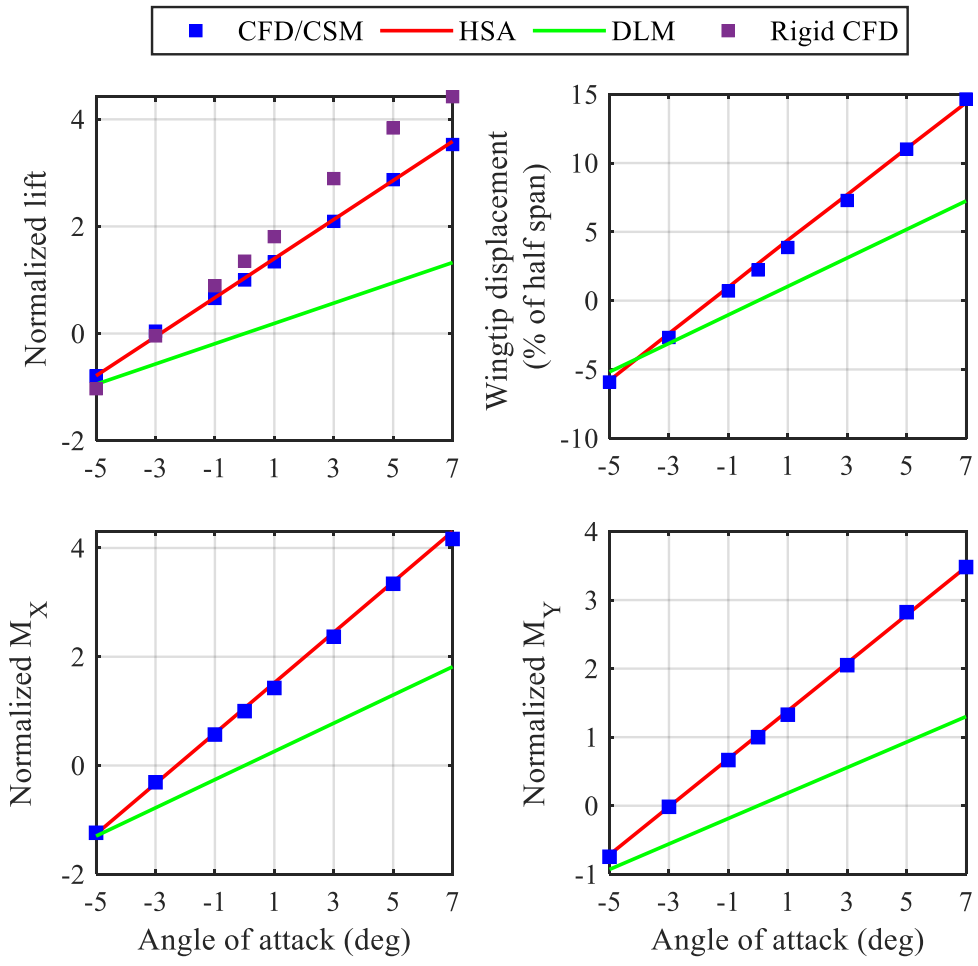

Figure 5: Coupled CFD-CSM compared against HSA and non-corrected DLM method.

When MLA and GLA are used during the wing sizing process, control effectiveness evaluation is critical. Because nonlinear effects can interfere with the control surfaces efficiency, it is important to use the right models. In his thesis, *Fillola* [5] showed that RANS CFD is accurate enough to achieve the aerodynamic characterisation of the ailerons and spoilers on an aircraft. The lift increment due to aileron rotation is compared between rigid CFD, and rigid DLM (no elastic effect) in Figure 6:

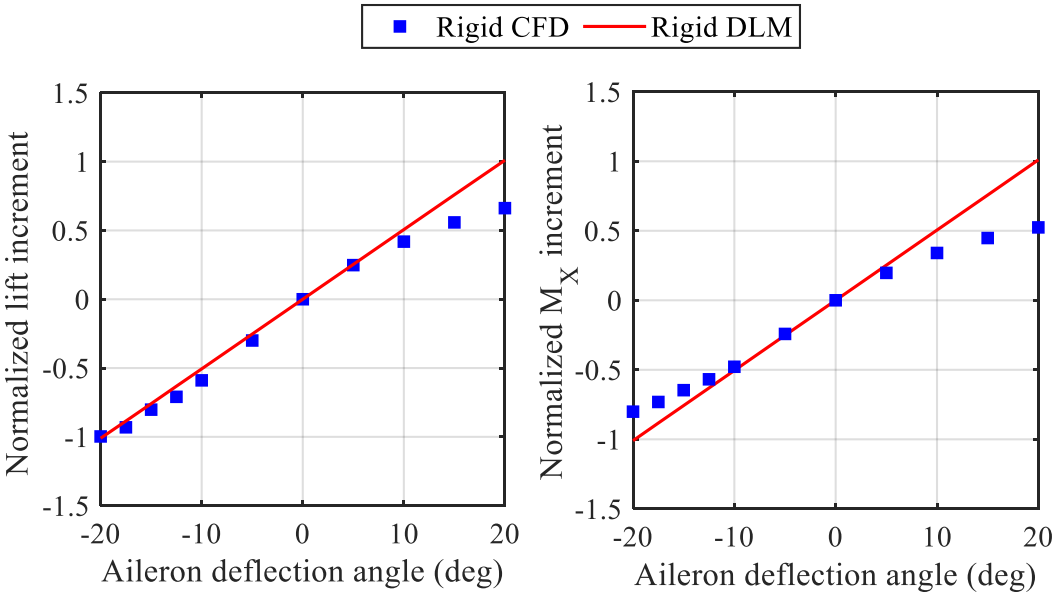

Figure 6: Aileron deflection lift increment from rigid CFD compared with rigid DLM panel method at Mach 0.85 and q = 15000 Pa and AoA = 0 degree.

DLM remains mostly accurate for negative deflection (aileron up) compared to the CFD. Nonetheless, it shows quite significant discrepancies at positive deflection (aileron down). This may be due to the linear panel method not being able to capture flow separation around the hinge of the aileron.

A comparison is made with a coupled CFD/CSM solution with a deflected aileron (as illustrated in Figure 7) and the NASTRAN HSA method combined with the aileron loads increments from rigid CFD. As for the previous results, the aircraft is flown at Mach 0.85 with a dynamic pressure of 15000 Pa.

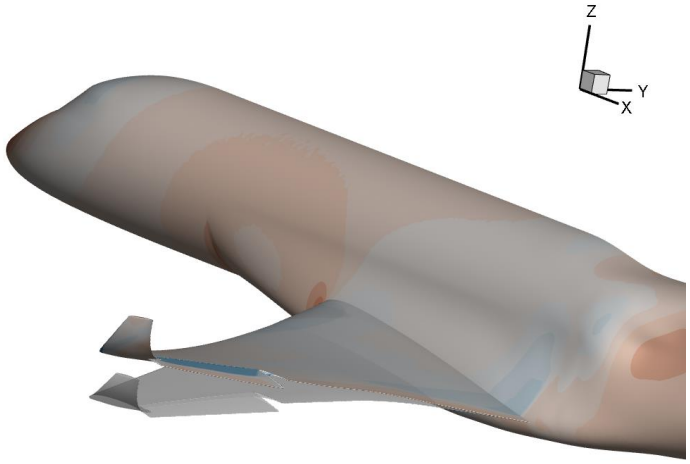

Figure 7: High fidelity aeroelastic coupled CFD/CSM simulation of the generic business jet.

The results shown in Figure 8 show a good agreement for all responses between the high fidelity coupled CFD/CSM solution and the HSA method running with NASTRAN. The error, however, tends to increase up to 10% when the aileron is deflected down at 15 degrees and the aircraft is at a high angle of attack (7 deg). As the HSA method remains a linear aerodynamic prediction method, it is not able to capture the incidence effect on the aileron load increment for the entire range of angle of attacks. Nonetheless, the technique remains accurate for most flight conditions and is very fast to compute compared to coupled CFD/CSM analysis.

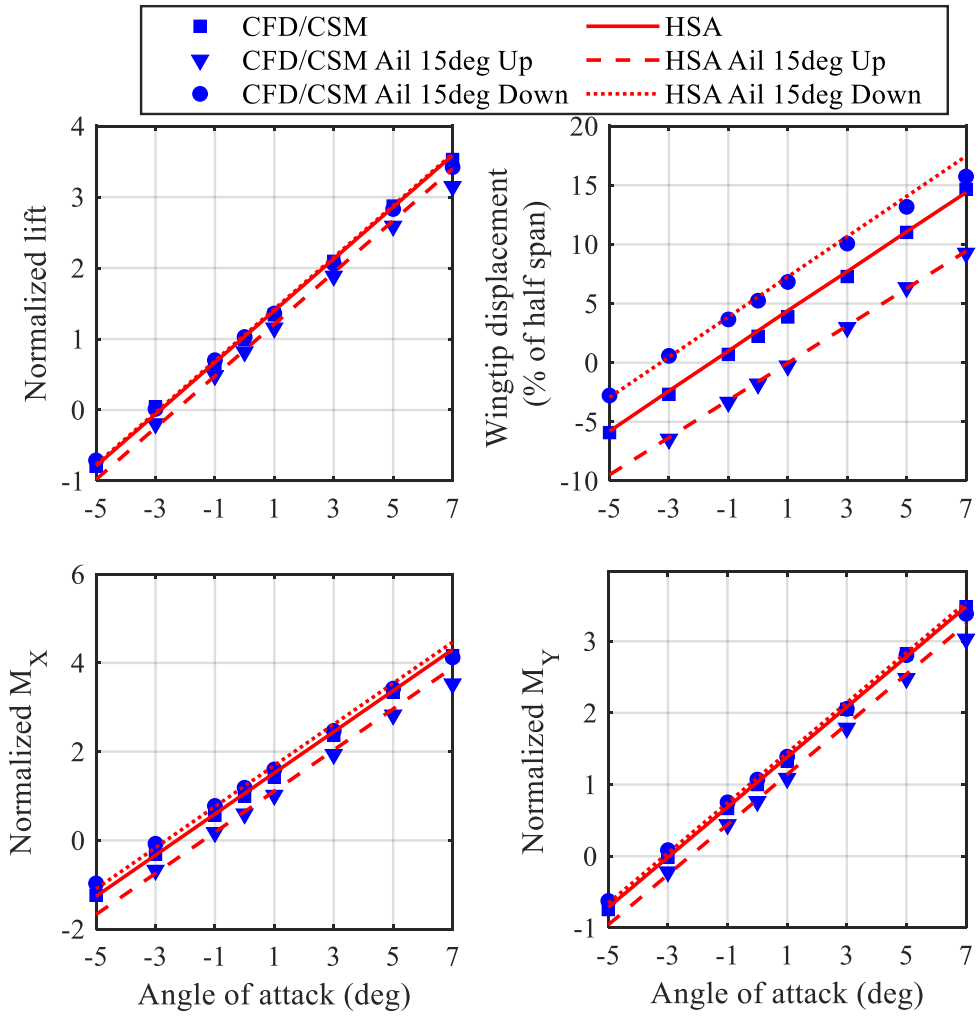

Figure 8: Coupled CFD-CSM compared against HSA with 0, +15 and -15 degrees of aileron deflection.

3 UNSTEADY AERODYNAMIC LOAD CORRECTION FOR THE WING AND MOVEABLE

In the previous section, it is shown that the aileron has a nonlinear behaviour; this also applies to its unsteady aerodynamic response. Achieving a correct is critical characterisation to obtain proper GLA performance estimation. The typical formulation of an aeroelastic system is defined by Equation 1 [6] $\Delta Q_e(s)$ and $\Delta Q_c(s)$ are the complex generalized incremental unsteady aerodynamic force coefficient due to elastic wing deformation and control surface deflection. $\{\xi(s)\}$ is the vector of n_s generalized structural displacement and q_∞ is the dynamic

pressure. $\{\delta_c(s)\}$ is the control surface commanded deflection. $[M]$ and $[K]$ are the generalized structural mass and stiffness matrices respectively.

$$([M]s^2 + [K]s + q_\infty[\Delta Q_e(s)])\{\xi(s)\} = -([M_c]s^2 + q_\infty[\Delta Q_c(s)])\{\delta_c(s)\} \quad (1)$$

In present work, the NASTRAN dynamic aeroelastic module (SOL146) [7] solves the system in the frequency domain. However, the aerodynamic loads due to the aileron deflection are included through time domain direct force input, which NASTRAN can convert to the frequency domain using Fourier Transform. A reduced order model (ROM) of the aileron unsteady aerodynamic behaviour generates the time-dependent forces and moments. The methodology used here is to derived transfer function from transient CFD simulations to evaluate the unsteady lift and moment characteristic of the moveable. As the transfer functions estimated are linear, look up tables are also used to approximate the steady, non-linear, forces and moments. Linear unsteady and non-linear steady loads contributions are summed up together, as shown in Figure 9. As for the HSA method, the set of look-up tables and transfer functions in the ROM are only valid for one flight point, and the rigid response of the control surface needs to be recomputed for different Mach and flight speeds.

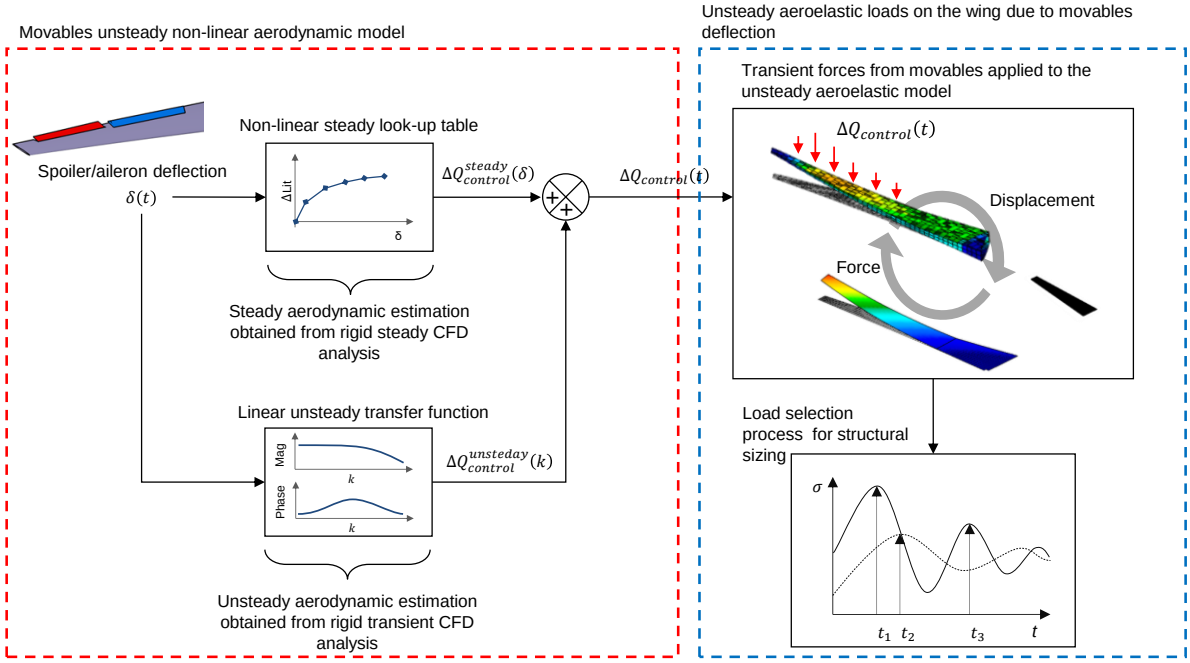

Figure 9: Schematic of the hybrid dynamic aeroelastic model.

Any control surfaces unsteady loads can be identified following the same process. The resulting forces and moments are then applied directly to the NASTRAN model during the dynamic aeroelastic simulation to simulate the effect of the GLA. On Figure 10 and Figure 11 is shown the resulting total lift of the aileron undergoing an arbitrary motion. The comparison is made between the ROM and transient rigid CFD analysis. The CFD simulation was executed using Ansys Fluent with a k-ω turbulence model and at Mach 0.85.

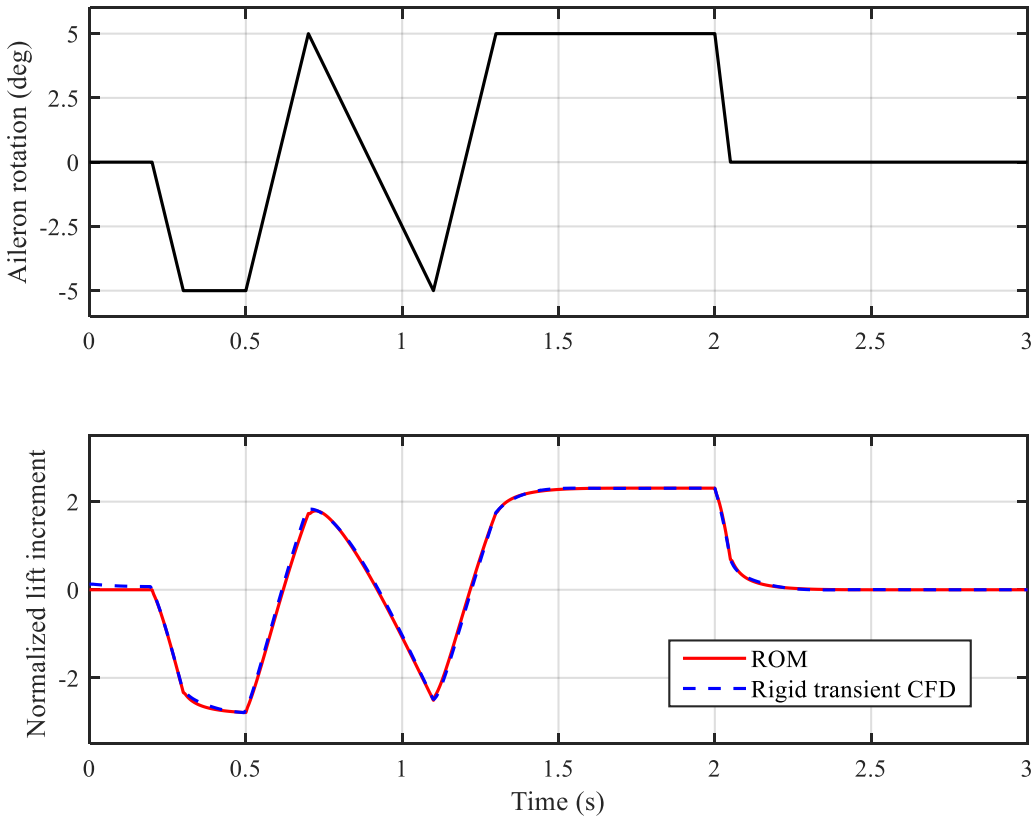

Figure 10: Comparison between the reference lift from the aileron using CFD and its approximation using the ROM.

A good agreement within 2% is achieved between the CFD simulation and the ROM when the aileron deflection does not exceed ± 5 degrees. The error goes up to 5% when the aileron is dynamically deflected to ± 10 degrees. This error is acceptable considering the flow non-linearity that starts to occur when aileron deflection reaches this angle.

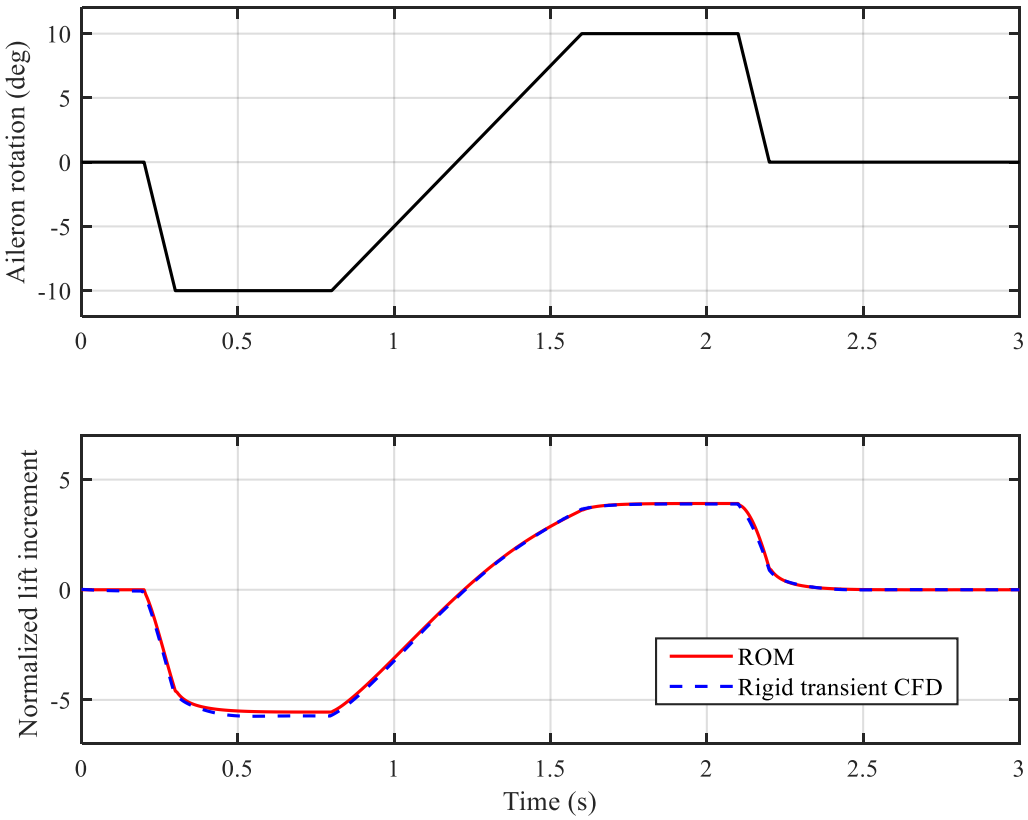

Figure 11: Comparison between the reference lift from the aileron using CFD and its approximation using the ROM.

The control surface ROM is then coupled to the aeroelastic NASTRAN solution. The aileron has a prescribed dynamic deflection, and the wing root moment M_X is recorded with the results shown in Figure 12. There are two distinct wings with different structural properties. Wing #1 is flexible with the first bending mode around 1.8Hz, while wing #2 has a stiffer structure, with a first bending mode around 6Hz. When the aileron loads are applied, it can be noticed that the response in M_X is much lower with wing #1. This is due to the aeroelastic behaviour of both respective wings, as a more flexible wing tends to have reduced aileron effectiveness.

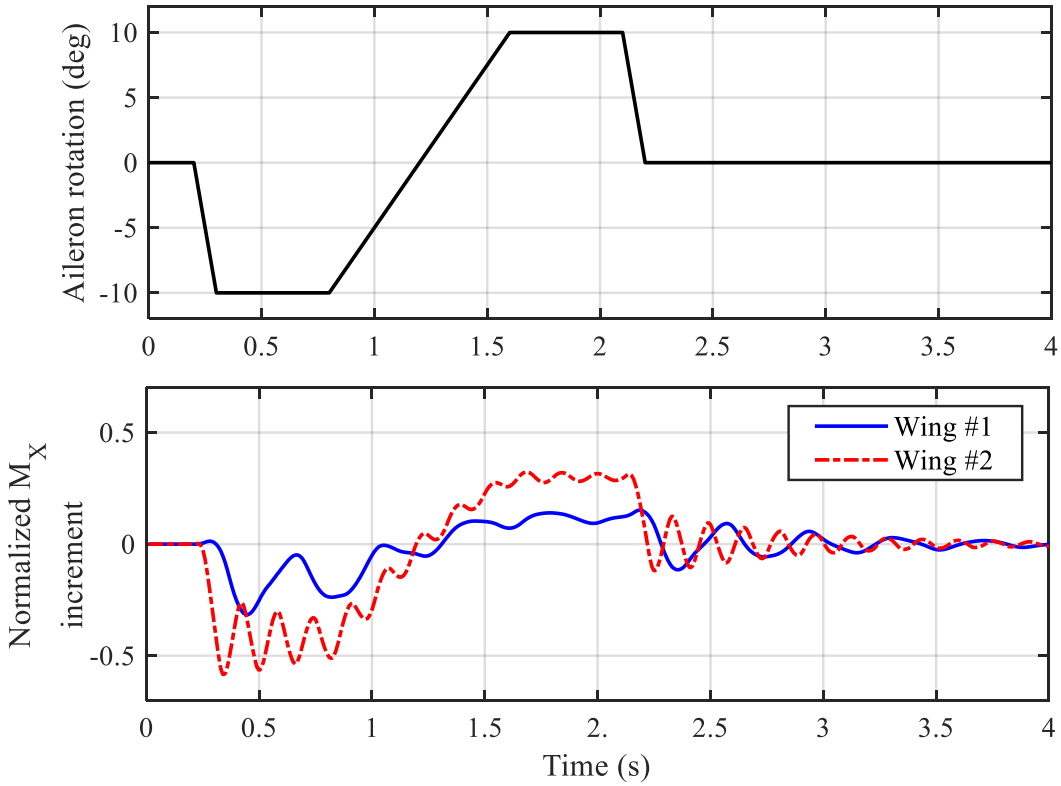

Figure 12: Incremental moment M_X due to rapid aileron deflection.

4 GUST LOAD HYBRID MODEL

Similarly to the aileron aerodynamic corrections, gust corrections are also approximated with a transfer function. Gust is considered as an external disturbance to the system, and hence, it is not dependent on the motion and vibration of the aircraft itself. The gust loads are computed from a transient CFD simulation on a fixed and rigid aircraft. *Raveh* [8] first described this approach.

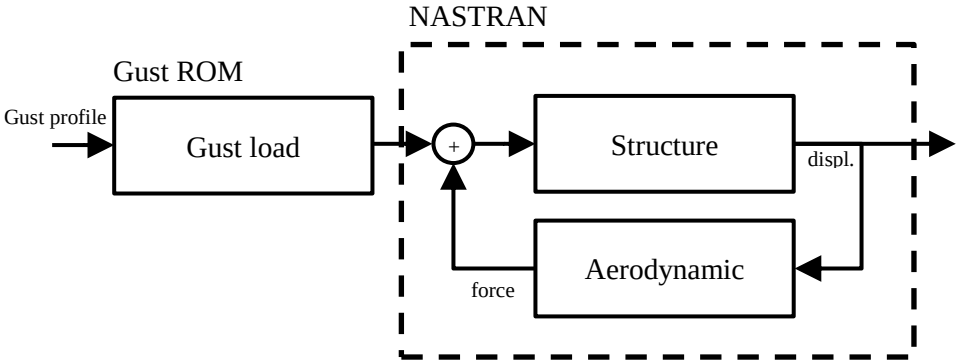

Figure 13: Schematic of the hybrid aeroelastic model with the gust loads computed from CFD derived transfer functions and the aeroelastic response evaluated with NASTRAN.

One challenging aspect of gust simulations using CFD with finite volumes is resolving the gust propagation, as it tends to numerically dissipate when travelling through the flow domain after being introduced from the boundaries. This issue is sometimes bypassed by prescribing the gust flow disturbance on every cell. This method, however, requires a low level of access to the CFD code and is not found possible with Ansys Fluent. Another solution is to resolve the gust

through the domain, but with a very fine mesh to avoid dissipation, making the simulation very computationally expensive. A third option is chosen here. It consists of running two gust simulations: one with the aircraft model where lift, moment and other unsteady loads are recorded during a gust encounter, and a second simulation, where the amplitude of the gust is characterised at the location of the aircraft model. The second simulation is done without the aircraft model. To ensure that the gust that "hits" the aircraft and the one that is recorded during the second simulation are identical, the same background structured mesh is used. This mesh is only 2 million cells and is shown in Figure 14. Thanks to the overset grid feature of Ansys FLUENT, a second more complex mesh with the aircraft is added when needed. This ensures a consistent gust propagation during both simulations. System identification of the gust loads is performed using a step profile gust. The comparison with the CFD and the identified gust transfer function is shown in with a good agreement.

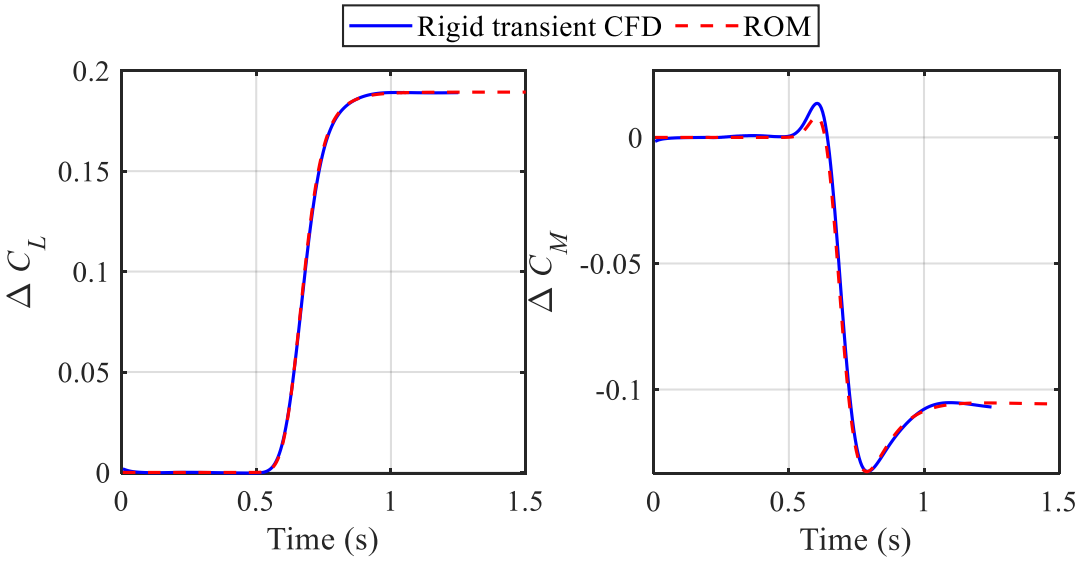

Figure 14: incremental lift and moment due to a step gust for response identification.

All the identified transfer functions are combined into a reduced order model of the aircraft (ROM). The gust load transfer functions can also be used to simulate continuous turbulence that would not be practical to do with conventional CFD method due to dissipation effects.

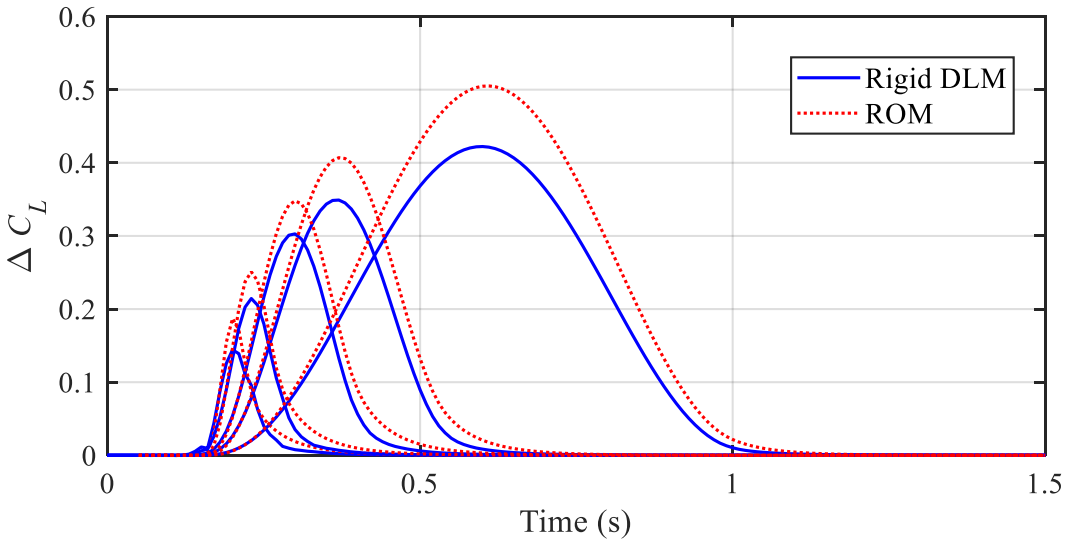

Figure 15: Rigid gust lift increment comparison between DLM and CFD.

When comparing the rigid lift increment due to gusts, we observe in Figure 15 that the CFD gives a larger amplitude compared to DLM. This observation is also made in the existing literature [9]–[11]. This translate into more significant incremental load factors and wing root bending moments on the flexible aircraft has seen in Figure 16.

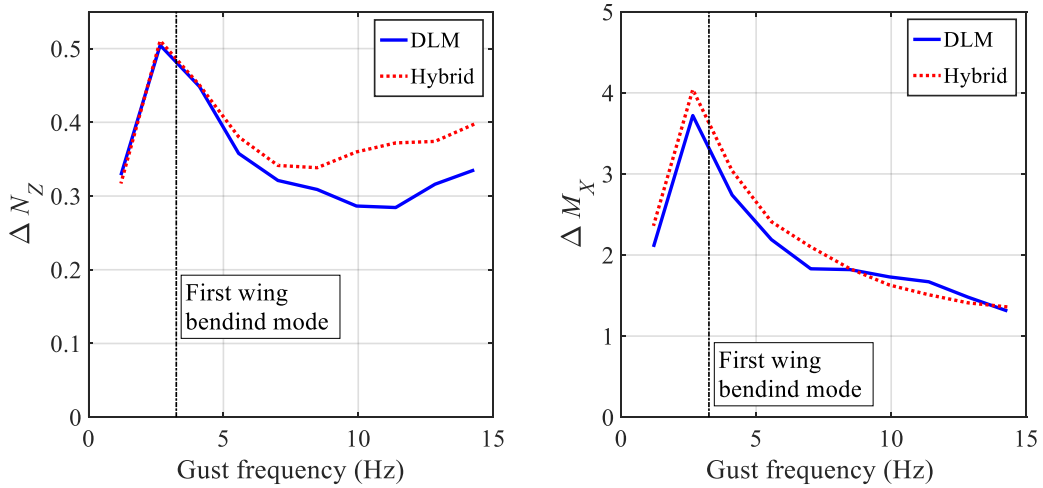

Figure 16: Loads comparison between the hybrid model and a purely DLM aeroelastic model.

Although the loads are more substantial in most scenarios, the overall time domain response stays similar between the hybrid model and the purely DLM aeroelastic simulation. Time response results are shown in Figure 17.

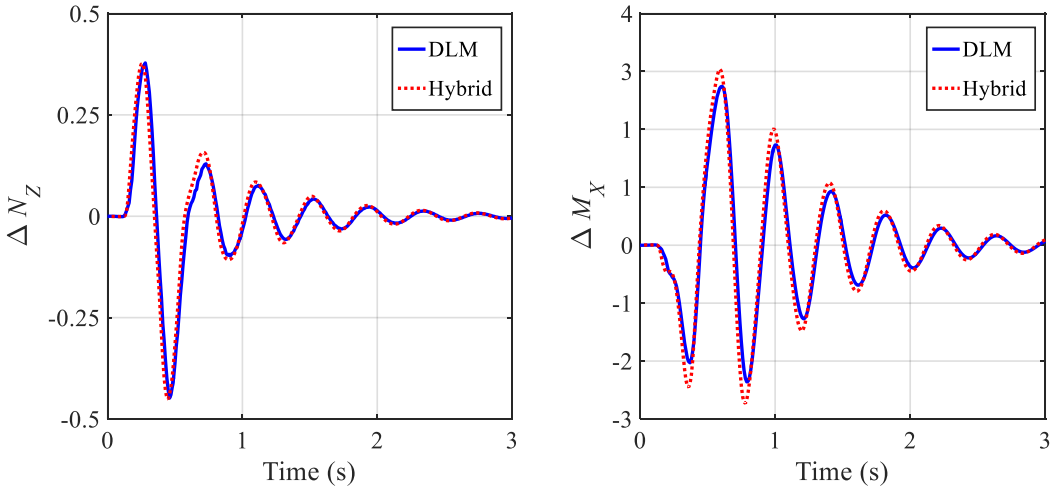

Figure 17: Time domain gust response on a flexible aircraft with the hybrid and the purely DLM aeroelastic model.

5 WING SIZING PROBLEM

The wing box optimisation strategy relies on the use of gradient-based algorithms. A gradient-based optimizer has the advantage to easily handle a high number of design variables, together with several loads cases and constraints. It is ideal for large structure sizing and is usually the centre-piece of any structural optimisation chain in both industrial and academic applications [12]–[14]. Aircraft structures are sized for multiple load cases which cover different flight regime in accordance with the certification authorities [15]. Loads must be provided for steady and dynamic conditions.

Including manoeuvres and gust load alleviation (MLA & GLA) in the wing-box sizing has potentially the advantage to decrease the wing box weight significantly thanks to a reduction of the loads. *Bordogna et al.* [16] have shown an increase of gust criticality when aggressive MLA setting is applied. Wing box optimisation was also performed with more futuristic configurations, using ailerons spanning the entire wing and showing significant flight performance improvements[17], [18]. *Wildschek et al.* [19] included a winglet tab for gust load alleviation purpose in the sizing process of a wing box using a feedforward controller. *Handojo et al.* [20] also included the GLA function in the sizing of a composite wing box and showed the effect of control delays on the resulting wing root loads. This optimisation was performed in a sequential manner with fixed control parameters. The same approach is used in this paper. *Bussemaker* [21] used a more integrated approach revolving around *Airbus Lagrange*, allowing concurrent optimisation of both control and structural parameters. This type of optimisation architecture is considered more efficient but complexify the use of multiple tools in the chain. It also requires full access to the code to compute the sensitivities efficiently.
In the following exercise and for the interest of time, only one flight point and fuel case are considered. Table 1 describes the parameters used for the problem.

Table 1: Wing sizing problem parameters

Aircraft parameters:
Mass case: MTOW
Dynamic pressure: 15000Pa
Mach: 0.85
Material: Aluminium
Load cases:
+2.5G pull-up and -1G push-down
10 positive and negative gust cases (+1G) from 9 to 107m
Optimisation parameters:
Design variable type: panel thickness
Design variable number: 65
Von Mises stress constraint
Plate buckling constraint
Objective: minimum weight

The optimisation process mostly relies on MSC NASTRAN SOL200 [22] for the structural optimisation and steady load analysis and SOL146 for the gust load analysis. Aerodynamic corrections are derived from rigid CFD-RANS simulations using Ansys Fluent. Matlab/SIMULINK connects all the different tools and runs both gust and control surfaces aerodynamic models.
Dynamic loads are usually a problematic type of load case to include in the optimisation. The sensitivities are more difficult to compute on transient responses and are demanding in term of CPU time. Only a hand few of aeroelastic sizing frameworks handle dynamic loads sensitivity analysis such as *Airbus Lagrange* [23] and *TU Delft Proteus* [24]. When using NASTRAN SOL200, such capability isn't available. *Stodieck et al.* [25] used finite difference approximations, to derive the gust response sensitivities externally. Another option is to decouple the response analysis from the structural sizing, and by updating the loads in a load loop. Skipping some of the sensitivities don't necessarily yield to the best optimum [26] but present the advantage to make the dynamic analysis code independent from the optimizer. The equivalent static loads (ESL) method formalised by *Kang et al.* [27] is used to bypass this issue and provides and a way to do structural optimisation with dynamic load cases.

Several studies are achieved with the framework introduced in this paper and are summarized in Figure 18. Firstly, the effect of steady load correction using the hybrid static approach is assessed. By using only DLM for load analysis, the optimised weight of the wing-box is about 5% lower than with the use of corrected loads and no gust. More interestingly, the parametric study using the aileron for MLA with DLM only ('HSA No') shows a very similar trend to the study with corrected loads ('HSA Yes'). The wing is mostly sized by the +2.5G pull-up when gust loads aren't applied, and the DLM aerodynamic prediction of the lift decrement generated by the ailerons deflecting upwards is actually very similar to the CFD prediction (as seen in Figure 6). This explains why the trends in weight reduction are similar.

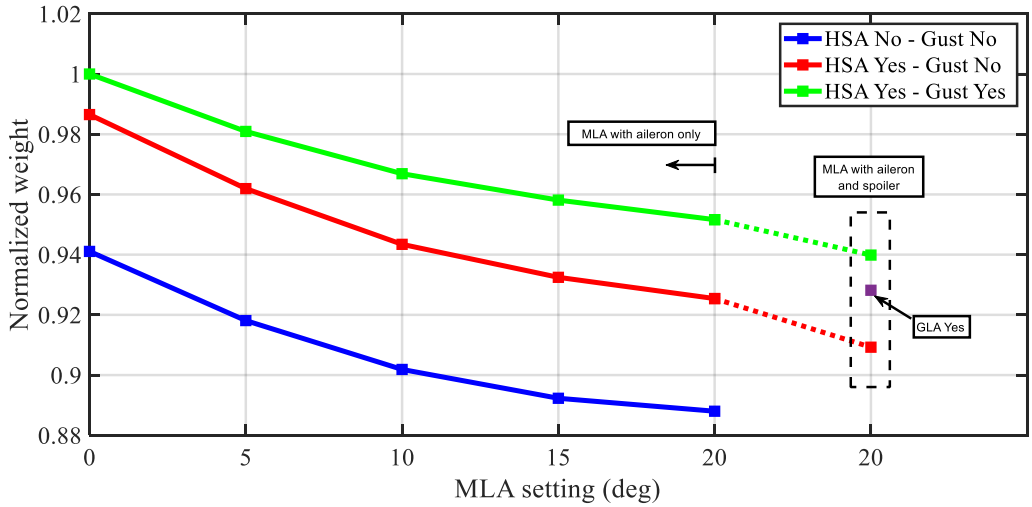

Figure 18: Normalized weights obtained from sizing the wing with different aerodynamic models and load alleviation setting. The aileron deflects upward during a pull-up and downward during a push-down.

When including the gust loads and the HSA correction, the effect of the MLA is limited to less than 5% with a 20 degrees aileron deflection (up during pull-up and down during push-down manoeuvres). Additional weight saving can be obtained when using the spoilers (also set to 20 degrees deflection). By deploying the outer spoiler during pull-up and the inner spoiler during push-down, the weight reduction from the baseline scenario can reach 6%. One of the most noticeable effects of alleviating manoeuvers loads is that gust loads became more critical. As shown in Figure 19, the maximum cutting loads in bending became driven by gust when using the MLA function (at 20 degrees aileron and spoiler deflection).

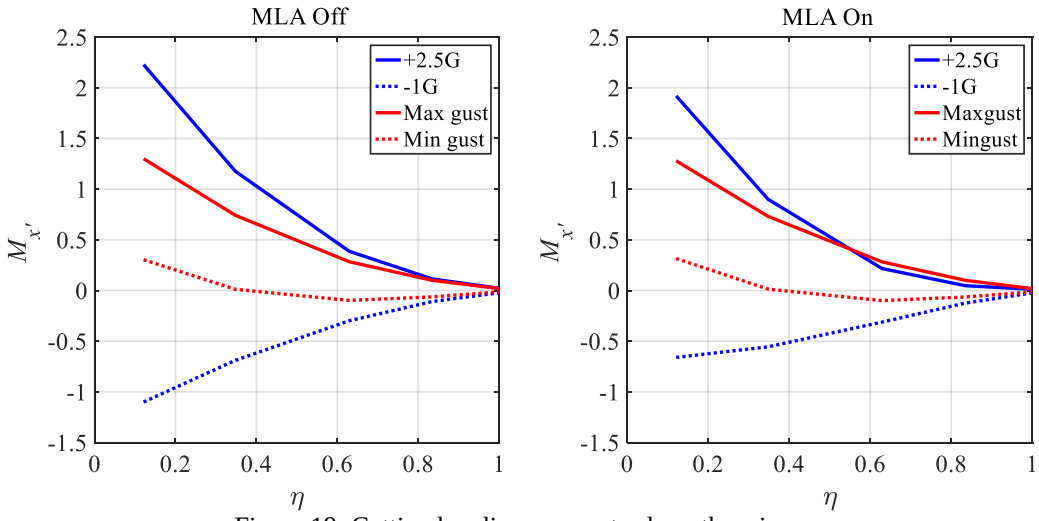

Figure 19: Cutting bending moments along the wingspan.

The same observation can be made between Figure 20 and Figure 21, were most critical responses (stress and buckling) are primarily caused by the gust loads when MLA is on. In addition, due to the reduction in wing skin thickness, most critical structural constraints are now in buckling rather than limit Von Mises stress.

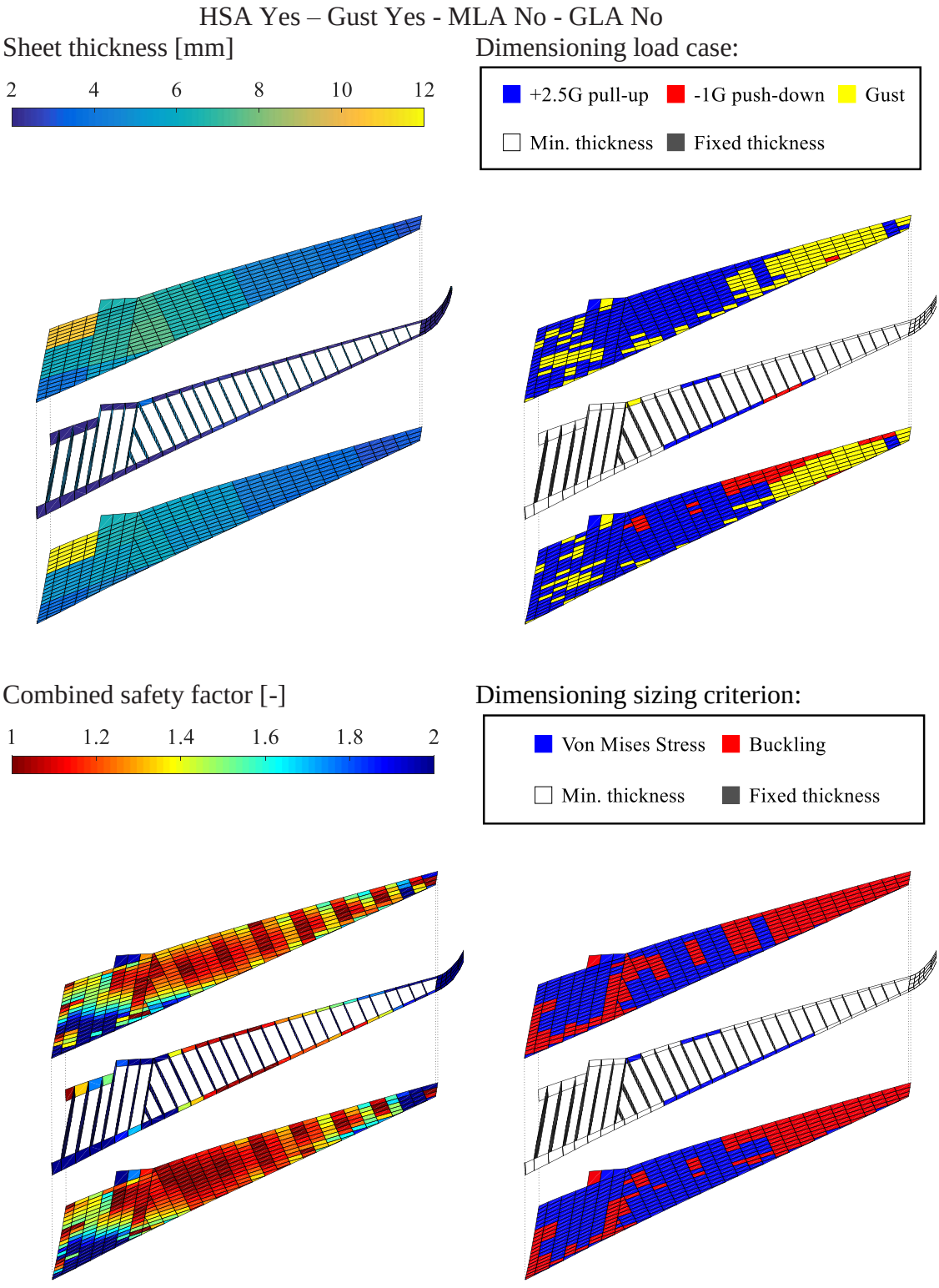

Figure 20: Optimised design obtained with the HSA correction and the gust loads. No alleviation function used.

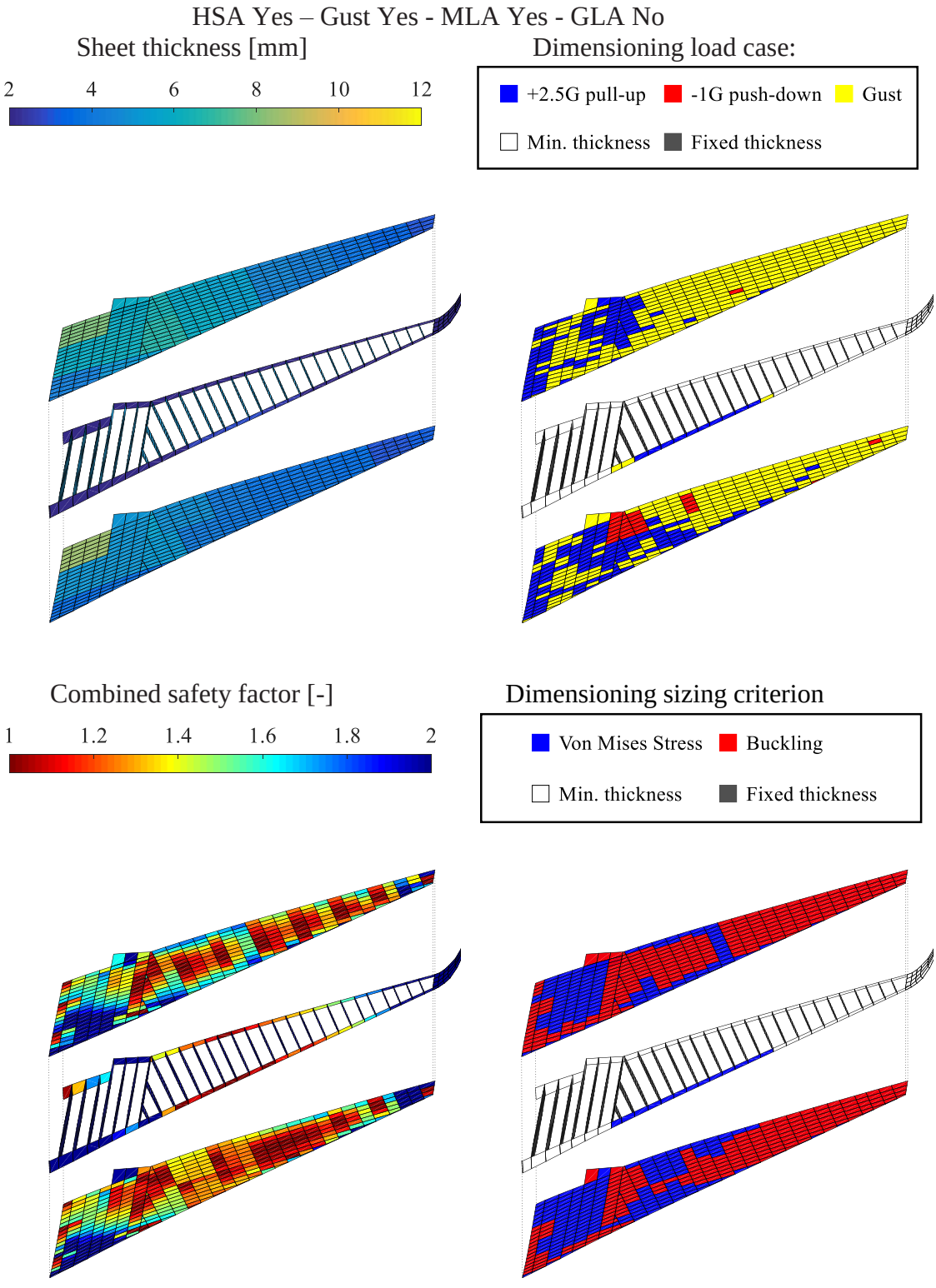

Figure 21: Optimised design obtained with the HSA correction and the gust loads. MLA with aileron and spoiler is used.

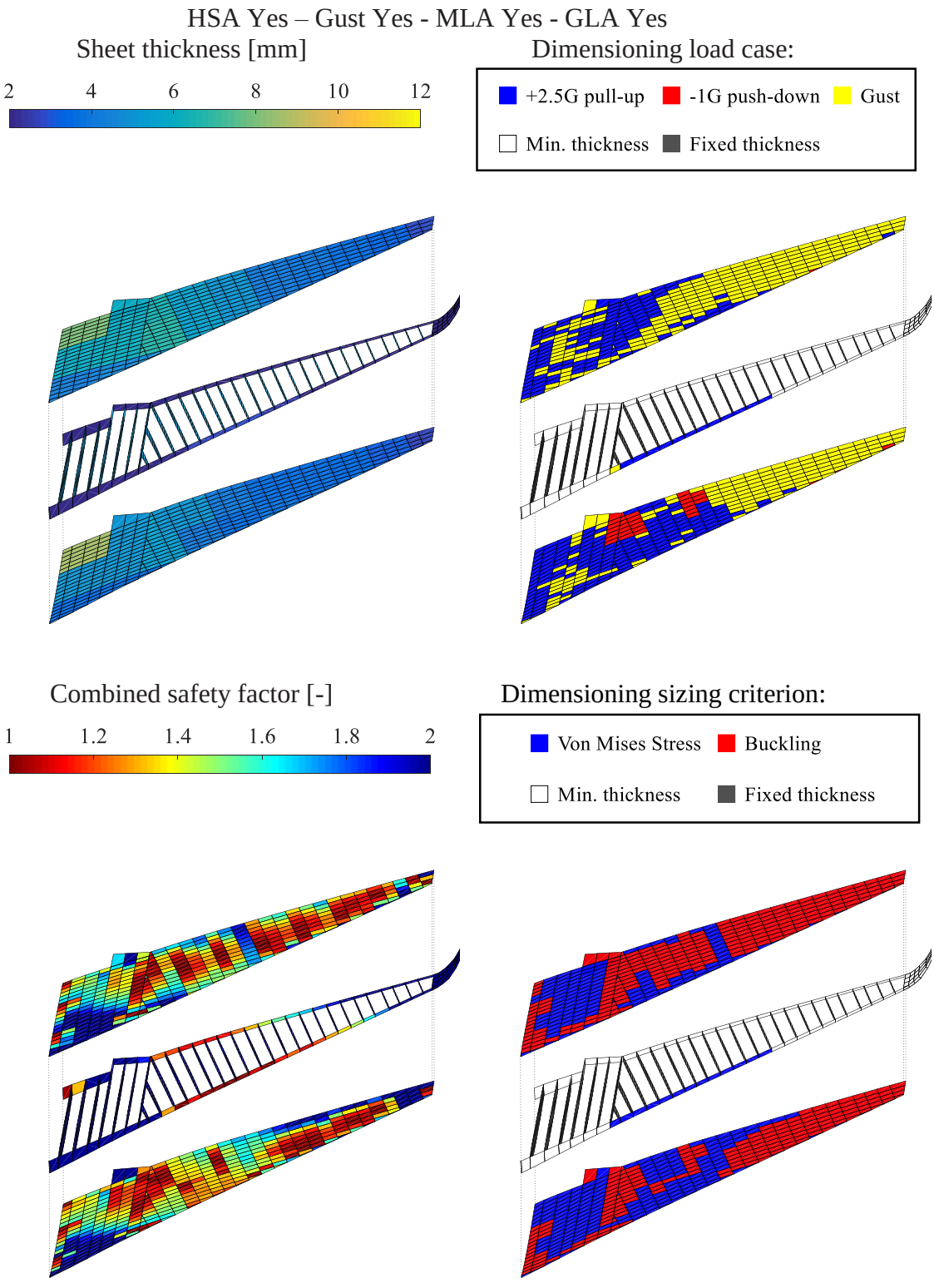

Figure 22: Optimised design obtained with the HSA correction and the gust loads. MLA with aileron and spoiler is used along with the GLA function (aileron only).

Finally, the impact of gust load alleviation on the aircraft weight is assessed. From Figure 18 we see that GLA can push the weight reduction from 6% to 7% when combined with an aggressive MLA strategy (aileron + spoiler). A simple proportional feed-forward controller is used to control the aileron motion during the gust encounter. Three parameters are used to design the controller: the gain of the controller to the incoming gust signal, the delay from the gust detection at the aircraft nose and the aileron maximum deflection speed.

A parametric study where the wing is resized for various combination of these parameters is achieved to find the best one. The best weight reduction is obtained with a controller having a delay of 100ms and a maximum deflection speed of 90 degrees. While these values seem reasonable, it is assumed that no additional lag exists in the actuation of the aileron. A delay of 200ms would result in no measurable weight reduction from the GLA.

As seen in Figure 23, the GLA system is able to reduce the gust loads at the tip of the aircraft, to a level where the cutting bending moments are similar to the manoeuvers ones. In addition, the GLA system is only useful up to 8Hz gusts. After this threshold, the incremental vertical load factor does not decrease. However, a substantial increase can be noticed at 1Hz. It is due to a limitation of the controller itself but it does not affect the final weight optimisation results, as the slowest gust is not sizing anyway. In Figure 22, it is observed that the GLA system reduces the criticality of gusts over the wing compared to the result obtained only with the MLA system.

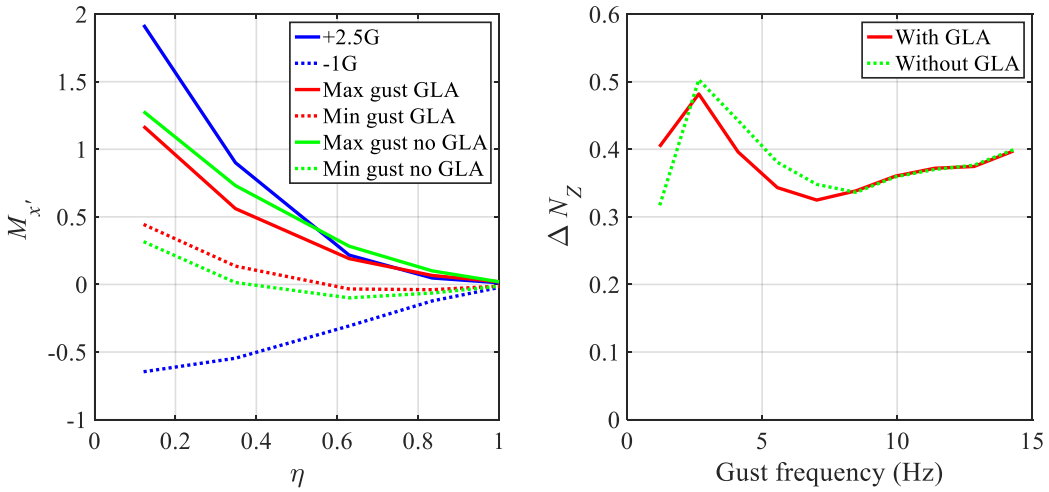

Figure 23: Cutting bending loads (left) and incremental load factor (right) with and without GLA during gust.

CONCLUSION

A methodology to size aircraft wing box accounting for the load alleviation functions of the control surfaces is presented. The overall optimisation remains mostly sequential, with the dynamic loads being updated using the equivalent static load approach.

The Hybrid Static Approach (HSA) is used to correct the steady wing and movable aerodynamic loads. It is validated against coupled CFD/CSM. The lift, root moments and maximum displacements comparisons show good agreements and generally do not exceed a 5% difference against the high fidelity method in most cases.

A method is developed for dynamic aileron loads too. It is based on transfer functions and lookup tables derived from CFD simulations. It is used to simulate movable loads to be supplied to a NASTRAN dynamic aeroelastic model. The ROM is compared against rigid transient CFD and gives good predictions.

A similar strategy is used to correct the gust loads. Corrected loads differ in amplitude from their panel linear potential flow counterpart. In the case of gust loads, the lift increment is higher using the CFD gust model. Ultimately, the methodology provides a good and consistent level fidelity for most important steady and dynamic load cases used in the sizing process.

The results of the wing sizing studies show how the corrected loads lead to a higher wing weight. The usage of aileron and spoiler for MLA and GLA help to reduce the wing weight up to 7%. Gust loads also became more critical, especially from the half span to the tip of the wing, when MLA is used.

Additional effects such as the aircraft incidence influence on the gust and control surfaces could also be implemented in the future. Along with additional load cases, failure scenario of one or several load alleviation systems on the aircraft may also be included in the sizing process, in order to determine a safe MLA/GLA budget when sizing the structure.

ACKNOWLEDGEMENT

This research is sponsored by the European Commission under the CleanSky II research program as part of project MANTA (Movables for next-generation aircraft) with Grant Agreement 724558.

BIBLIOGRAPHY

[1] J. K. S. Dillinger, M. M. Abdalla, Y. M. Meddaikar, and T. Klimmek, “Static aeroelastic stiffness optimization of a forward swept composite wing with CFD-corrected aero loads,” *CEAS Aeronaut. J.*, pp. 1–18, May 2019.

[2] MSC Software, F. G. Di Vincenzo, and A. Castrichini, “MSC Nastran Hybrid Static Aeroelasticity Integrated, Accurate Static Aeroelastic Analysis with CFD data,” 2013.

[3] M. T. Bordogna, D. Bettebghor, C. Blondeau, and R. De Breuker, “Surrogate-based aerodynamics for composite wing box sizing,” *17th Int. Forum Aeroelasticity Struct. Dyn.*, 2017, Como, Italy.

[4] G. Schewe and H. Mai, “Influence of flexibility on the steady aeroelastic behavior of a swept wing in transonic flow,” *J. Fluids Struct.*, vol. 81, pp. 255–269, Aug. 2018.

[5] G. Fillola, “Etude expérimentale et simulations numériques d’écoulements autour de surfaces mobiles de voilure.”, Université de Toulouse, 2006

[6] M. Karpel, B. Moulin, and P. C. Chen, “Dynamic Response of Aeroservoelastic Systems to Gust Excitation,” *J. Aircr.*, vol. 42, no. 5, pp. 1264–1272, 2005.

[7] E. H. Johnson and W. P. Rodden, “MSC Nastran Version 68 Aeroelastic Analysis User’s Guide,” *MSC Softw. Aeroelastic Guid.*, 1994.

[8] D. E. Raveh, “CFD-Based Models of Aerodynamic Gust Response,” Journal of

Aircraft, Volume 44, Number 3, May 2007.
[9] N. Kroll *et al.*, "DLR project Digital-X: towards virtual aircraft design and flight testing based on high-fidelity methods," *CEAS Aeronaut. J.*, vol. 7.
[10] F. Huvelin, P. G. Lavigne, and C. Blondeau, "High fidelity numerical simulations for gust response analysis.", 13th International Forum on Aeroelasticity and Structural Dynamics, Bristol, Great Britain, 2013.
[11] D. E. Raveh, "CFD-Based Gust Response Analysis of Free Elastic Aircraft," ASDJournal, vol. 2, no. 1, pp. 23–34, 2010.
[12] P. Piperni, A. DeBlois, and R. Henderson, "Development of a Multilevel Multidisciplinary-Optimization Capability for an Industrial Environment," *AIAA J.*, vol. 51, no. 10, pp. 2335–2352, Oct. 2013.
[13] S. M. Meldrum, L. Colo, G. Broux, and E. Garrigues, "A New Dassault Industrial Approach For Aero-Structural Optimization Of Composite Structures With Stacking Table Constraints," *17th Int. Forum Aeroelasticity Struct. Dyn* 2017, Como, Italy.
[14] F. Hürlimann, R. Kelm, M. Dugas, K. Oltmann, and G. Kress, "Mass estimation of transport aircraft wingbox structures with a CAD/CAE-based multidisciplinary process," *Aerosp. Sci. Technol.*, vol. 15, no. 4, pp. 323–333, Jun. 2011.
[15] European Aviation Safety Agency, "Cs25," no. July, p. 1037, 2012.
[16] M. T. Bordogna, P. M. G. J. Lancelot, D. Bettebghor, and R. De Breuker, "Aeroelastic tailoring for static and dynamic loads with blending constraints," *17th Int. Forum Aeroelasticity Struct. Dyn.*, 2017, Como, Italy.
[17] B. K. Stanford, "Optimal Control Surface Layout for an Aeroservoelastic Wingbox," *AIAA J.*, vol. 55, no. 12, pp. 4347–4356, Dec. 2017.
[18] E. P. Krupa, J. E. Cooper, A. Pirrera, and R. Nangia, "Improved aerostructural performance via aeroservoelastic tailoring of a composite wing," *Aeronaut. J.*, vol. 122, no. 1255, pp. 1442–1474, Sep. 2018.
[19] A. Wildschek, "Concurrent Optimization of a Feed-Forward Gust Loads Controller and Minimization of Wing Box Structural Mass on an Aircraft with Active Winglets," in *16th AIAA/ISSMO Multidisciplinary Analysis and Optimization Conference*, 2015.
[20] V. Handojo, P. Lancelot, and R. De Breuker, "Implementation of Active and Passive Load Alleviation Methods on a Generic mid-Range Aircraft Configuration," in *2018 Multidisciplinary Analysis and Optimization Conference*, 2018.
[21] J. H. Bussemaker, "Wing Optimization with Active Load Control," 2018.
[22] MSC Software, "MSC Nastran 2012 Design Sensitivity and Optimization User ' s Guide," 2012.
[23] G. Schuhmacher, F. Daoud, Ö. Petersson, and M. Wagner, "Multidisciplinary Airframe Design Optimisation." 28th Congress of the International Council of the Aeronautical Sciences, ICAS 2012, 23-28 September 2012, Brisbane, Australia.
[24] D. Rajpal, E. Gillebaart, and R. De Breuker, "Preliminary aeroelastic design of composite wings subjected to critical gust loads," *Aerosp. Sci. Technol.*, 2018.
[25] O. Stodieck, J. E. Cooper, P. M. Weaver, and P. Kealy, "Aeroelastic Tailoring of a Representative Wing Box Using," Journal of Aircraft, vol. 55, no. 4, 2017.
[26] M. Stolpe, A. Verbart, S. Rojas-Labanda, M. Stolpe matst, dtudk Alexander Verbart, and S. Rojas-Labanda srla, "The equivalent static loads method for structural optimization does not in general generate optimal designs," *Struct. Multidiscip. Optim.*, vol. 58, pp. 139–154, 2018.
[27] B. . Kang, W. . Choi, and G. . Park, "Structural optimization under equivalent static loads transformed from dynamic loads based on displacement," *Comput. Struct.*, vol. 79, no. 2, pp. 145–154, Jan. 2001.

COPYRIGHT STATEMENT